Acoustic detection of the magnetocaloric effect: Application to Gd and $Gd_{5.09}Ge_{2.03}Si_{1.88}$

A. O. Guimarães,* M. E. Soffner, A. M. Mansanares,† and A. A. Coelho
Instituto de Física Gleb Wataghin, Universidade Estadual de Campinas (UNICAMP), CP 6165, 13083-970 Campinas, SP, Brazil

A. Magnus G. Carvalho and M. J. M. Pires
Instituto Nacional de Metrologia, Normalização e Qualidade Industrial (INMETRO), 25250-020, Duque de Caxias, RJ, Brazil

S. Gama
Departamento de Ciências Exatas e da Terra, Universidade Federal de São Paulo (UNIFESP), 09972-270, Diadema, SP, Brazil

E. C. da Silva
Laboratório de Ciências Físicas, Universidade Estadual do Norte Fluminense Darcy Ribeiro, 28013-602, Campos dos Goytacazes, RJ, Brazil

(Received 16 July 2009; published 7 October 2009)

In this paper we present a simple method for the determination of the total magnetocaloric effect based on the acoustic detection of the adiabatic temperature rise caused by the application of an ac magnetic field of small amplitude. The continuous scanning of a superimposed dc magnetic field allows, by numerical integration, the determination of large temperature variations caused by magnetic field steps from zero to tens of kOe. Absolute values of temperature rise are easily acquired after the calibration of the microphone signal using an appropriate reference sample. Once the calibration is done, no further information about the sample's thermal properties is necessary since the measured signal is directly proportional to the temperature variation. Measurements were made in Gd and $Gd_{5.09}Ge_{2.03}Si_{1.88}$ samples in the temperature range from 240 to 320 K. The technique shows to be suitable for the investigation of materials undergoing both purely magnetic phase transitions, as in the case of Gd, and magnetic-crystallographic first-order ones, as observed for $Gd_{5.09}Ge_{2.03}Si_{1.88}$. Besides the ability to determine the temperature variation due to a large magnetic field step through the continuous scanning of the magnetic field, the technique is also very suitable for measuring the magnetocaloric effect under very small magnetic field steps since it has sensitivity below millikelvin. Moreover, it is able to detect temperature variations in very small amount of sample, leading to its potential application in magnetocaloric thin films.

DOI: 10.1103/PhysRevB.80.134406 PACS number(s): 75.30.Mb, 75.30.Kz, 75.50.Cc

I. INTRODUCTION

The magnetocaloric effect (MCE) was discovered in 1881 and consists in the heating or cooling of a magnetic material under the action of a magnetic field. In the recent past the MCE has been of great interest due to its potential application in refrigeration systems, with the replacement of conventional gas cycles by magnetic cycles. The effect is characterized both through the adiabatic temperature change under magnetic field variation, ΔT_S, and by means of the isothermal entropy change, ΔS_T. It can be measured directly through the temperature rise of the sample due to a magnetic field step, or it can be calculated from magnetization and heat-capacity data as a function of temperature and magnetic field.[1–4]

A prototype material for room-temperature refrigeration is gadolinium, which orders magnetically at $T_C \sim 290$ K. Recently, a series of $Gd_5(Si_xGe_{1-x})_4$ alloys has been widely investigated, mainly after 1997, when Pecharsky and Gschneidner[5] reported the discovery of large entropy changes in $Gd_5Si_2Ge_2$, the so-called giant magnetocaloric effect. Compositions in the range $0.24 < x < 0.5$ present a first-order transition, which consists of simultaneous crystallographic change and magnetic ordering in a reversible way.

The search for magnetocaloric materials has been increasing, with a consequent demand for their characterization. For the MCE determination, the direct measurement of the temperature rise is certainly important. Furthermore, a noncontact technique is even more important for this purpose. The acoustic detection of the MCE accomplishes these desirable characteristics and it was first proposed by Otowski *et al.*[6] in 1993. It is similar to the photoacoustic technique, with the thermal wave being generated by the adiabatic application of a modulated magnetic field superimposed to a static one. The small field variation (tens of Oe) produces a temperature rise in the sample, which originates the pressure increase in a closed cell. This acoustic wave is detected by a microphone and an appropriate calibration procedure provides the modulated temperature rise values. Rather than focusing on the effects of small temperature oscillations δT, the technological interest in magnetocaloric materials involves large temperature variations ΔT_S caused by large magnetic field steps ΔH from zero to tens of kOe. The total MCE, i.e., the MCE for large magnetic field variation, was derived by Gopal *et al.*[7] for Gd, Gd-Dy, and Gd-Er, using acoustic measurements and magnetization data of the samples.

In this paper, we present a simple method for the determination of the total MCE based on the direct integration of the modulated temperature variation acoustically detected. The key issue of the method is the continuous scanning of the static magnetic field, from zero to 50 kOe. This method may be used in both paramagnetic and ferromagnetic tem-

perature ranges as well as around the transition temperature in which the maximum MCE occurs. Besides, after the calibration procedure, no additional data is required. We investigated samples of Gd and $Gd_{5.09}Ge_{2.03}Si_{1.88}$, in the temperature range from 240 to 320 K.

II. ACOUSTIC DETECTION

The photoacoustic technique is based on the detection of acoustic waves produced in a closed cell using a microphone. For solid samples, the absorption of intensity modulated light heats up the sample and the temperature oscillations on its surface reach the adjacent gas layer, which expands and works as a gas piston generating pressure waves.[8] For a fixed modulation frequency, the acoustic signal, S_{ac}, is given by

$$S_{ac} = G(T)F_{sys}\delta T \tag{1}$$

in which $G(T)$ is a temperature-dependent factor carrying information about the gas properties, F_{sys} depends on the electronics of the detection system, and δT is the complex temperature oscillation at the sample surface. The temperature oscillation depends on the optical and thermal properties of the samples, besides light intensity and modulation frequency.

The acoustic measurement of the MCE is based on the same principles of the photoacoustic technique. However, in this case the temperature oscillation of the sample is produced by the application of a modulated (ac) magnetic field of small amplitude (tens of Oe). This ac magnetic field is superimposed on a static (dc) one. Therefore, such magnetoacoustic signal can be written as in Eq. (1) and a suitable calibration procedure can be used to eliminate the $G(T)F_{sys}$ factor in order to allow the absolute determination of the modulated temperature rise δT.

For this purpose, first we have determined the temperature dependence of the cell, $G(T)$, using an electrical resistance inside it as a heat source (Joule effect). Modulated current at a fixed frequency was applied keeping the electrical power constant while scanning the temperature. The further step was to determine the F_{sys} factor by comparing the measured signal to the calculated MCE values (δT) for a reference sample.

Considering the temperature T as a function of the magnetic field H and the entropy S of the system, the adiabatic temperature rise due to the MCE, δT_S, can be expressed as a function of the ac magnetic field applied to the sample, δH, as

$$\delta T_S = \left(\frac{\partial T}{\partial H}\right)_S \delta H = \beta \delta H \tag{2}$$

and using the Maxwell relation $(\partial S/\partial H)_T = (\partial M/\partial T)_H$ we find[4]

$$\delta T_S = -\frac{T}{C_H}\left(\frac{\partial M}{\partial T}\right)_H \delta H. \tag{3}$$

In the above equations M is the total magnetization (total magnetic moment) and C_H is the heat capacity of the sample at magnetic field H. Therefore, the temperature oscillation can be calculated for a reference sample since C_H and M are known as functions of H and T. Comparing Eqs. (2) and (3), we see that the adiabatic magnetocaloric coefficient, β, is given by $\beta = -(T/C_H)(\partial M/\partial T)_H$.

However, as mentioned in the introduction, the interest concerning magnetocaloric materials involves the adiabatic temperature variation ΔT_S due to large magnetic field steps. In this sense, we present here a simple way to determine the total MCE from the sum of several δT_S quantities acoustically detected. From the experimental curves of δT_S vs H a finite temperature variation ΔT can be found, as follows:

$$\Delta T = \int_0^{H_f} \delta T_S = \int_0^{H_f} \beta dH = \frac{1}{\delta H}\int_0^{H_f} \delta T_S dH. \tag{4}$$

It has to be noticed that the temperature oscillation, obtained from the acoustic measurements, δT_S, is indeed adiabatic since the modulation period (on the order of ms) is much smaller than the typical thermal diffusion time (on the order of hundreds of ms). However, the integration path in Eq. (4) is along an isothermal magnetic field scan. There is, therefore, an error if ΔT is regarded as the finite temperature increase for a single magnetic field step from zero to H_f. This error can be estimated from the acoustic measurement data at several temperatures and magnetic fields, and it is of a few percent, as it will be demonstrated bellow.

Finally, it is important to stress that the acoustic detection of the MCE, i.e., the measurement of δT_S, does not present any restriction related to discontinuities in the thermodynamic functions in the vicinity of first-order phase transitions. This is because the temperature variation in the sample is directly probed by the microphone. Moreover, the calibration procedure necessary for the determination of the absolute values, which is described below, can be done using a reference material that presents a second-order phase transition, such as gadolinium, in a temperature range slightly above the phase-transition temperature, thus avoiding any difficulty due to singularities or discontinuities in the thermodynamic functions.

III. MATERIALS

Recently, intermetallic compounds of the $Gd_5(Si_xGe_{1-x})_4$ family received much attention. The most prominent property of this family of compounds is the giant magnetocaloric effect occurring slightly below room temperature for $x=0.5$. Compounds with such stoichiometry present a simultaneous magnetic (ferromagnetic to paramagnetic) and structural (orthorhombic to monoclinic) first-order transition. The transitions can be induced by temperature, magnetic field, or pressure.[9–11]

Usually these compounds are obtained in arc furnaces in inert atmosphere and are thermally treated, seeking for the desired phase purity. It is common, however, the formation of other phases besides the one with the nominal stoichiometry, even after careful treatment.[12] This happens mainly when samples are prepared with the nominal stoichiometries in the range of occurrence of the monoclinic phase

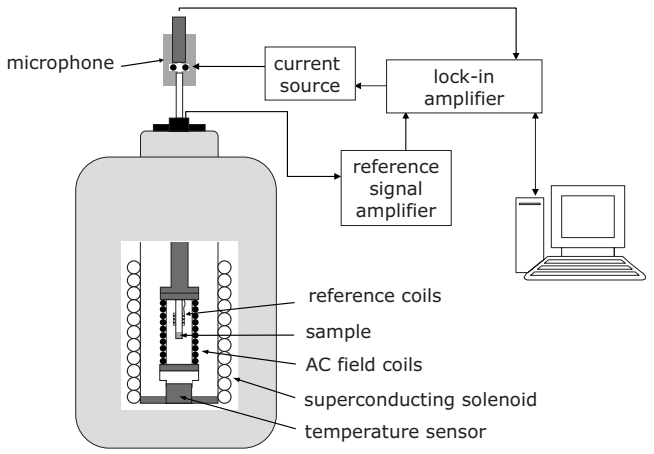

FIG. 1. Diagram of the experimental arrangement.

$(0.24 \leq x \leq 0.5)$. Two phase transitions occurring in temperatures relatively close to each other have been reported in several works on samples with such a multiphase composition. Usually one of the transitions is of first-order type and the other is of second-order type.[5,13] As $Gd_5(Si_xGe_{1-x})_4$ are promising compounds for room-temperature magnetic refrigeration, it is important to know how sensitive and accurate the acoustic detection technique presented here is when applied to these multiphase samples.

The pure Gd (reference sample for calibration) and $Gd_{5.09}Ge_{2.03}Si_{1.88}$ were the materials studied in the present work. Commercial 99.9 wt % Gd and electronic grade Si and Ge were used in the preparation of the samples. The Gd powder sample used for calibration was obtained by filing the material with grains smaller than 50 μm. The measured T_C for the Gd powder was 288 K, below the corresponding transition temperature found for the bulk material. A possible cause for such decrease in the T_C value is the stress arising from the filing. The $Gd_{5.09}Ge_{2.03}Si_{1.88}$ sample was arc melted three times in Ar atmosphere, inverting the ingot position each time. About 5 g of material was melted and the lost of material during the preparation is negligible. The resulting as-cast sample was polycrystalline and very brittle. The powder sample, with grains smaller than 50 μm, was prepared by hand grinding the bulk material. The nominal stoichiometry was $Gd_{5.09}Ge_{2.03}Si_{1.88}$ but metallographic analysis, magnetometry, and electron-spin resonance show that the sample is composed of at least two phases. The results of these three techniques are very similar to the ones obtained for other samples prepared in the same conditions.[11,13,14] For those samples a majority phase with the composition $Gd_{5.09}Ge_{2.03}Si_{1.88}$ and a Si rich minority phase have been identified. Therefore, for simplicity, in the text this sample is referred as $Gd_{5.09}Ge_{2.03}Si_{1.88}$ sample.

IV. EXPERIMENTAL SETUP

Figure 1 shows a diagram of the experimental arrangement used for the acoustic detection of the MCE. An acoustic cell was placed in a Quantum Design® physical properties measurement system (PPMS), which is a general purpose temperature and magnetic field platform used for magnetic, thermal, and transport properties measurements. The dc magnetic field is generated by a superconducting solenoid in a liquid-helium Dewar and the insert for susceptibility measurements provides the ac field. The temperature and the magnetic field are controlled by an external console.

The acoustic cell consists of a cylindrical quartz tube with 2.0 mm inner diameter and 1.0 m length having a closed bottom end where the sample is held. The top part of the tube is connected to a Sennheiser microphone which is kept out of the Dewar to avoid pick up signals due to the magnetic fields. The tube is placed in the Dewar through a drilled flange sealed by an O-ring to maintain vacuum in the PPMS inner chamber. The microphone signal is lock-in analyzed (Stanford SR830). The reference signal for the synchronous amplification is provided by a coil located around the quartz tube.

In order to determined the temperature dependence of the cell, $G(T)$, a constant power heat source was provided by a 10 Ω resistance (coil) placed in the microphone holder. Modulated current of a few mA was delivered by a controlled current source (see Fig. 1).

Measurements were performed by scanning the dc magnetic field from 0 to 50 kOe in 25 min and recording the data every 30 Oe. The alternating magnetic field was 30 Oe peak to peak with a modulated frequency of 270 Hz, fulfilling the adiabatic condition. This modulation frequency is not far from one of the acoustic resonances of the cell, ensuring a good signal/noise ratio. The temperature was controlled within 0.05 K in the range from 240 to 320 K.

V. RESULTS AND DISCUSSION

Figure 2 shows the amplitude of the magnetoacoustic signal for Gd as a function of the magnetic field for temperatures from 252 to 316 K. At lower temperatures (ferromag-

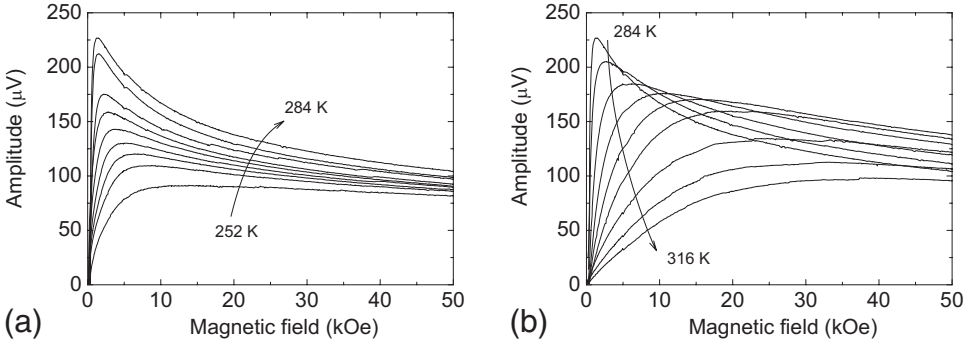

FIG. 2. Magnetoacoustic signal for Gd as a function of the dc magnetic field for temperatures (a) below and (b) above 284 K. Curves are separated by 4.0 K temperature increment.

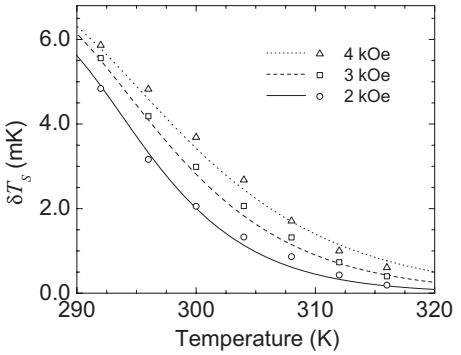

FIG. 3. Calculated δT_S (peak-to-peak) curves for Gd at three dc magnetic fields in the paramagnetic temperature range, for an ac magnetic field of 30 Oe peak to peak. Symbols represent experimental magnetoacoustic data after calibration.

netic temperature range), far from the magnetic transition, the signal amplitude saturates for magnetic fields higher than 10 kOe. As temperature increases nearing the magnetic transition, the signal amplitude passes through a maximum value at magnetic fields of a few kOe and then diminishes to some extent. The peak value grows up monotonically until 284 K, near the magnetic phase-transition temperature, and falls back as the transition is reached and surpassed. The magnetic field in which the peak occurs is reduced until 284 K, reaching a minimum value of about 2 kOe, and then increasing again as the temperature reaches the paramagnetic range. Finally, in the paramagnetic temperature range the signal amplitude shows a smooth rise when increasing the magnetic field. The magnetoacoustic signal phase remains constant along the magnetic field scan for all temperatures (not shown).

The behavior described above is consistent with the fact that the $(\partial M/\partial T)_H$ is maximum at T_C for low values of magnetic field. As a general behavior, $(\partial M/\partial T)_H$ diminishes for a given temperature when the magnetic field is increased. It also diminishes for a given magnetic field when the temperature is shifted out of the temperature transition. In other words, despite the changes in the heat capacity near T_C, which certainly influences the magnetoacoustic signal, it seems that the overall behavior of the signal is dominated by $(\partial M/\partial T)_H$.

In order to determine the adiabatic temperature rise, δT_S, which produces the magnetoacoustic signal shown in Fig. 2, the measured signal amplitude of Gd was properly normalized by the temperature response of the cell, $G(T)$. After this, the normalized signal was fitted, using the minimum square method, to the calculated adiabatic temperature rise for Gd in the temperature range from 290 to 320 K, for three values of the dc magnetic field (2–4 kOe) and an ac magnetic field of 30 Oe peak to peak. The chosen temperature range for this calibration procedure corresponds to the Gd paramagnetic range in which the changes on the heat capacity are small for the used dc fields. For the calculated δT_S, the average value of the specific heat of (280 ± 20) J/kg K was used for the entire temperature range and magnetic fields chosen for the calibration. This value was obtained from literature data[2,15–17] and checked with thermal diffusivity measurements of the reference sample using the photoacoustic technique at zero magnetic field. The values of $(\partial M/\partial T)_H$ used in such calculation were obtained from magnetization measurements performed in a Quantum Design® superconducting quantum interference device magnetometer. Figure 3 shows the calculated adiabatic temperature rise curves and the experimental points from the magnetoacoustic signal after normalization and best data fitting. The data-fitting output gives the constant F_{sys} value which is used to transform every magnetoacoustic signal presented henceforth into temperature rise, δT_S. As we can see, the temperature rise is on the order of a few millikelvin for an ac magnetic field of 30 Oe.

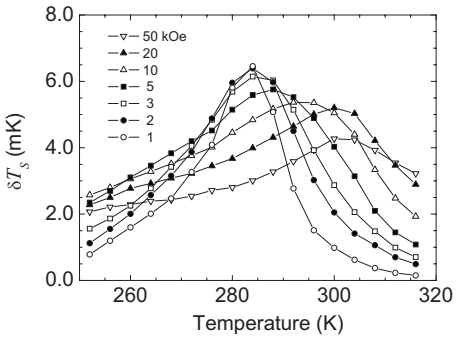

FIG. 4. Modulated magnetocaloric effect, δT_S, versus temperature for Gd measured with different dc magnetic fields.

Now using the $G(T)F_{sys}$ factor, the adiabatic temperature rise for each measurement can be recovered, as a function of T and H. Figure 4 presents such data obtained from the measurement on Gd of Fig. 2 as a function of temperature for several values of the dc magnetic field. In this graph we can see a broadening of the curves as the magnetic field increases, as well as a reduction in the maximum δT_S value. It is observed also a shift of the maximum δT_S to higher temperatures, as a consequence of the displacement of the transition temperature. Again, we can say that the shape of the curves is mainly governed by $(\partial M/\partial T)_H$ in dealing with a second-order transition, which was also reported in Refs. 6 and 18. Figure 5 presents a complete map of δT_S versus T and $\log(H)$ in which the shift of the peak to higher temperatures is clearly seen when the magnetic field increases.

The numerical integration above described [Eq. (4)] was performed based on the curves of Fig. 2 after the correction by the $G(T)F_{sys}$ factor and the results are plotted in Fig. 6.

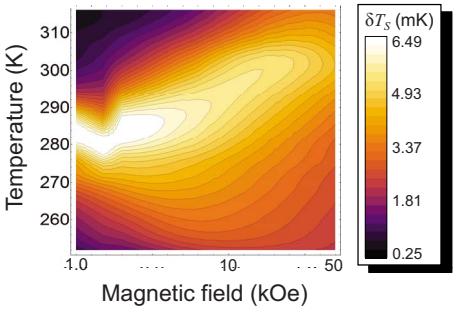

FIG. 5. (Color online) Map of the modulated magnetocaloric effect, δT_S, for Gd. Horizontal axis presents the magnetic field in a logarithmic scale.

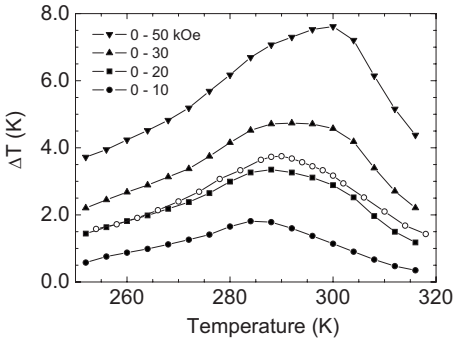

FIG. 6. Total magnetocaloric effect, ΔT, versus temperature for Gd measured using acoustic detection for several magnetic field steps (solid symbols). Results of a direct measurement are shown for 20 kOe magnetic field step (open symbols).

The solid symbols represent the total MCE, ΔT, determined using the acoustic detection for several magnetic field steps. In addition, the temperature rise in a 1.0 g Gd bulk sample, located in the PPMS inner chamber, was measured by a Cernox sensor, properly calibrated. The results of such a conventional direct measurement are also shown in Fig. 6 for a zero to 20 kOe field step (open symbols). Besides the good agreement with the conventionally measured MCE, the results obtained by the acoustic detection are consistent with data reported in literature for Gd, concerning both the shape and the magnitude of the curves.[7,17]

Figure 7 shows the curves of δT_S for the $Gd_{5.09}Ge_{2.03}Si_{1.88}$ sample as a function of the dc magnetic field for some representative temperatures. The curves at 240 and 315 K are similar to the curves of Gd in the ferromagnetic and paramagnetic regimes, respectively. However, the other two curves are quite different from those expected for materials which undergo a purely magnetic second-order phase transition, as observed for Gd (see Fig. 2). Indeed, $Gd_{5.09}Ge_{2.03}Si_{1.88}$, which is actually the majority phase of the sample, undergoes a magnetic-crystallographic first-order phase transition at 270 K. As mentioned above, the sample also presents a minority phase, which is rich in Si and that undergoes a magnetic second-order phase transition at 300 K.[14] Therefore, at intermediate temperatures, between 270 and 300 K, there is coexistence of the $Gd_{5.09}Ge_{2.03}Si_{1.88}$ paramagnetic phase and the minority ferromagnetic one. The

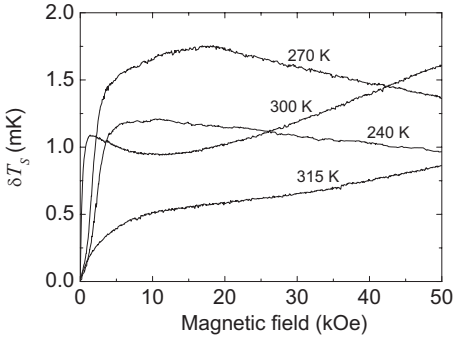

FIG. 7. Modulated magnetocaloric effect, δT_S, for $Gd_{5.09}Ge_{2.03}Si_{1.88}$ as a function of the dc magnetic field for several temperatures.

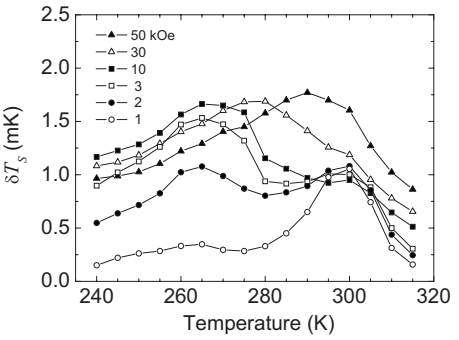

FIG. 8. Modulated magnetocaloric effect, δT_S, versus temperature for $Gd_{5.09}Ge_{2.03}Si_{1.88}$ measured with different dc magnetic fields.

peak for low magnetic field observed in the 300 K curve in Fig. 7 is related to the second-order phase transition.

Figure 8 presents δT_S as a function of the temperature for several dc magnetic fields while Fig. 9 shows a complete map of δT_S versus T and $\log(H)$. The shape of the curves clearly reveals the occurrence of two phase transitions. At low magnetic fields δT_S has a maximum around 300 K. This peak gets wider at higher magnetic fields, similar to the case of Fig. 4. For the first-order phase transition, however, δT_S is very small for fields lower than 2 kOe, despite the abrupt changes observed in the magnetization. This is certainly caused by the influence of the heat capacity, which peaks around the transition temperature,[5,19] thus reducing the temperature variation in the sample. Increasing the magnetic field, δT_S becomes prominent, with a peak that shifts from 265 K to higher temperatures at high magnetic fields. This is clearly seen in the map of Fig. 9.

The total MCE, ΔT, for the $Gd_{5.09}Ge_{2.03}Si_{1.88}$ sample is calculated and plotted, for several magnetic field steps, in Fig. 10. In each curve one can see two maxima associated to the two phase transitions. The main shape of the curves is in agreement with results in literature for multiphase materials.[5,20] The maximum value of ΔT observed at 270 K for a magnetic field step from 0 to 50 kOe indicates that the giant effect observed for the isothermal entropy change, ΔS_T, is not converted into a giant temperature variation for our as-cast sample. This is in contrast with some results in the literature calculated from heat-capacity data and in the same direction of other reported direct measurements.[20–22] It is im-

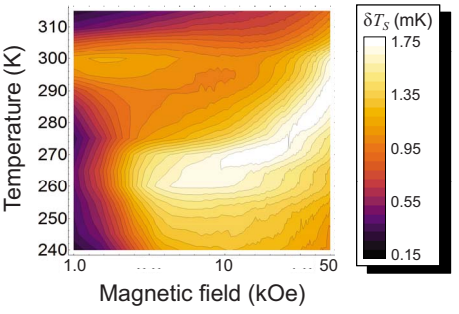

FIG. 9. (Color online) Map of the modulated magnetocaloric effect, δT_S, for $Gd_{5.09}Ge_{2.03}Si_{1.88}$. Horizontal axis presents the magnetic field in a logarithmic scale.

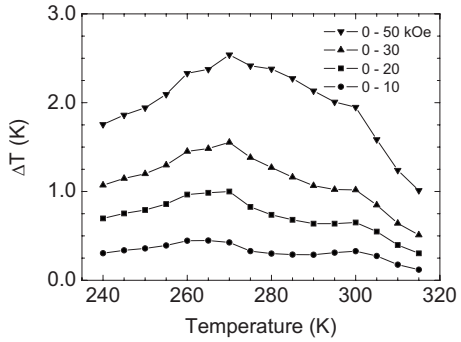

FIG. 10. Total magnetocaloric effect, ΔT, versus temperature for $Gd_{5.09}Ge_{2.03}Si_{1.88}$ measured using acoustic detection and calculated for several magnetic field steps.

portant, however, to point out that for materials undergoing first-order phase transitions, the MCE is strongly dependent on the sample preparation. Gschneidner *et al.*,[23] for instance, reported differences higher than 30% for the maximum MCE comparing two samples from different batches of alloys with the same starting stoichiometry.

On the difference between ΔT and ΔT_S

As commented above, the integration path in Eq. (4) is along an isothermal magnetic field scan, resulting in a difference between the obtained value of ΔT using this method and the adiabatic temperature change, ΔT_S, under magnetic field variation. Considering Eq. (2), one can see that the acoustic signal, after normalization and calibration, finally delivers the adiabatic magnetocaloric coefficient, $\beta(T,H)$. This coefficient represents the slope of the adiabatic curves in a T vs H diagram, i.e., $\beta=(\partial T/\partial H)_S$ as written in Eq. (2). The adiabatic temperature change, ΔT_S, can be obtained by integrating β along one specific adiabatic curve. On the other hand, ΔT results from the integration of β along an isothermal path [see Eq. (4)].

Departing from a given point $(T_0,\ H=0,\ S_0)$ in the T vs H diagram, a family of adiabatic curves is crossed along an isothermal path following the increasing magnetic field, as depicted in the inset of Fig. 11. Therefore, the used value of $\beta(T_0,H)$ in Eq. (4) does not correspond to S_0 anymore but to another adiabatic curve at T_0, a lower temperature value than that of S_0 for the same magnetic field. Considering $\delta\theta$ the temperature difference between these two adiabatic curves at a given magnetic field, the deviation introduced in the value of β is written as

$$\beta(H)_{S_0} - \beta(H)_{T_0} = \left(\frac{\partial \beta}{\partial T}\right)_H \delta\theta. \tag{5}$$

The quantity $(\partial\beta/\partial T)_H$ can be calculated from the magnetoacoustic signal itself by taking the values of β at two distinct adjacent temperatures. Figure 11 shows the calculated curves of $(1/\beta)(\partial\beta/\partial T)_H$ as a function of the magnetic field for Gd at 300 K and for $Gd_{5.09}Ge_{2.03}Si_{1.88}$ at 270 K, temperatures at which the value of ΔT was maximum for a magnetic field step from 0 to 50 kOe. By integrating Eq. (5) along the magnetic field range, the difference $(\Delta T_S - \Delta T)$ is found. A rough estimation of this difference can be get using the average values of $(1/\beta)(\partial\beta/\partial T)_H$ and $\delta\theta$. The average values of $(1/\beta)(\partial\beta/\partial T)_H$, taken along the entire range of magnetic field, are $-2\%\ K^{-1}$ for Gd and $-1\%\ K^{-1}$ for $Gd_{5.09}Ge_{2.03}Si_{1.88}$. Using 50% of ΔT for the magnetic field step from 0 to 50 kOe as the average $\delta\theta$ along the entire magnetic field range, the error is estimated to be of 8% for Gd and of 1.3% for $Gd_{5.09}Ge_{2.03}Si_{1.88}$.

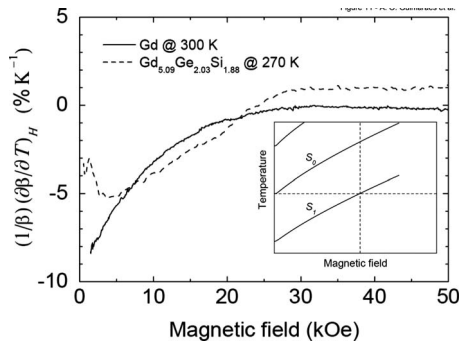

FIG. 11. Calculated curves of $(1/\beta)(\partial\beta/\partial T)_H$ for Gd at 300 K and for $Gd_{5.09}Ge_{2.03}Si_{1.88}$ at 270 K, as a function of the magnetic field. The insert illustrates a family of adiabatic curves in a T vs H diagram.

VI. CONCLUSIONS

In this paper, we presented results on the MCE in Gd and $Gd_{5.09}Ge_{2.03}Si_{1.88}$ obtained using acoustic detection for continuous scanning of the magnetic field. The measurements are reproducible and an appropriate calibration procedure leads to temperature rise in Gd consistent with results previously reported. For the $Gd_{5.09}Ge_{2.03}Si_{1.88}$ sample, the curves of δT_S clearly show the two expected phase transitions. Furthermore, the behavior of δT_S, mainly for low dc magnetic field strengths, allows one to distinguish a second-order phase transition from a first-order magnetic-crystallographic one in which the influence of the specific heat is pronounced, thus reducing the MCE.

The numerical integration proposed permits the ΔT determination for several magnetic field steps and the results for Gd are in agreement with the literature and with a conventional direct measurement. Although the comparison between ΔT values for the $Gd_{5.09}Ge_{2.03}Si_{1.88}$ sample and literature is not straightforward, the shape of the curves agree with the observed MCE for multiphase materials in which the two phase transitions are easily identified for low magnetic field steps, becoming superimposed to each other for higher magnetic field steps. This is due to the drastic shifting at the first-order transition temperature, especially for high magnetic field strengths.

The method is suitable for the measurement of the MCE, without any restriction concerning the nature of the phase transition. The technique presents good sensitivity, being able to detect spurious material phase, and it is particularly applicable to investigate the effect in low magnetic fields. Besides, the advantage of the noncontact approach, with the air as the transducer, allows the MCE detection for low-mass

samples, which is severely limited in conventional measurements when sample and sensor have similar heat capacities. In this sense, there is a clear possibility of using the acoustic detection to study magnetocaloric thin-film systems in which there is an increasing interest nowadays.

The uncertainties involving the acoustic detection are satisfactorily compared to conventional methods. Simple repetitions of the measurements for the same sample results in deviations smaller than 2%, caused mainly by noise and the reproducibility of the overall experimental conditions. Since the modulation frequency for the ac field is not far from an acoustic resonance frequency of the cell, changes in the gas volume in the cell, due to changes in the sample's volume, produce changes in the measured signal, which was properly evaluated by varying the amount of sample. The last important source of error remains in the uncertainty in the specific-heat value used for calibration, which is of 7% in our case. Considering all these sources, the errors in the acoustically detected MCE measurements are estimated in 15–20 %, which is of the same order of those in conventional methods. Finally, it has to be observed that the accurate value of the ac magnetic field, δH, is necessary only to the correct determination of δT_S, the modulated temperature which causes the acoustic signal. In the determination of ΔT, all that is needed is the adiabatic magnetocaloric coefficient, β, which can be determined after the calibration provided all the experimental conditions are kept unchanged, including δH.

ACKNOWLEDGMENTS

Authors acknowledge the Brazilian agencies FAPESP, CNPq and CAPES, and FAEPEX-Unicamp for financial support.

*Present address: Laboratório de Ciências Físicas, Universidade Estadual do Norte Fluminense Darcy Ribeiro, 28013–602, Campos dos Goytacazes, RJ, Brazil.

†manoel@ifi.unicamp.br

[1] M. Foldeaki, W. Schnelle, E. Gmelin, P. Benard, B. Koszegi, A. Giguere, R. Chahine, and T. K. Bose, J. Appl. Phys. **82**, 309 (1997).

[2] V. K. Pecharsky and K. A. Gschneidner, Jr., J. Appl. Phys. **86**, 565 (1999).

[3] B. R. Gopal, R. Chahine, and T. K. Bose, Rev. Sci. Instrum. **68**, 1818 (1997).

[4] V. K. Pecharsky and K. A. Gschneidner, Jr., J. Magn. Magn. Mater. **200**, 44 (1999).

[5] V. K. Pecharsky and K. A. Gschneidner, Jr., Phys. Rev. Lett. **78**, 4494 (1997).

[6] W. Otowski, C. Glorieux, R. Hofman, and J. Thoen, Thermochim. Acta **218**, 123 (1993).

[7] B. R. Gopal, R. Chahine, M. Földeàki, and T. K. Bose, Rev. Sci. Instrum. **66**, 232 (1995).

[8] A. Rosencwaig and A. Gersho, J. Appl. Phys. **47**, 64 (1976).

[9] V. K. Pecharsky and K. A. Gschneidner, Jr., Adv. Mater. **13**, 683 (2001).

[10] P. J. von Ranke, N. A. de Oliveira, and S. Gama, J. Magn. Magn. Mater. **277**, 78 (2004).

[11] A. M. G. Carvalho, C. S. Alves, A. Campos, A. A. Coelho, S. Gama, F. C. G. Gandra, P. J. von Ranke and N. A. Oliveira, J. Appl. Phys. **97**, 10M320 (2005).

[12] A. O. Pecharsky, K. A. Gschneidner, Jr., and V. K. Pecharsky, J. Magn. Magn. Mater. **267**, 60 (2003).

[13] S. Gama, C. S. Alves, A. A. Coelho, C. A. Ribeiro, A. I. C. Persiano, and D. Silva, J. Magn. Magn. Mater. **272-276**, 848 (2004).

[14] M. J. M. Pires, A. M. G. Carvalho, S. Gama, E. C. da Silva, A. A. Coelho, and A. M. Mansanares, Phys. Rev. B **72**, 224435 (2005).

[15] C. Glorieux, J. Thoen, G. Bednarz, M. A. White, and D. J. W. Geldart, Phys. Rev. B **52**, 12770 (1995).

[16] G. Bednarz, D. J. W. Geldart, and M. A. White, Phys. Rev. B **47**, 14247 (1993).

[17] S. Yu. Dan'kov, A. M. Tishin, V. K. Pecharsky, and K. A. Gschneidner, Jr., Phys. Rev. B **57**, 3478 (1998).

[18] C. Glorieux, J. Caerels, and J. Thoen, J. Appl. Phys. **80**, 3412 (1996).

[19] V. K. Pecharsky and K. A. Gschneidner, Jr., J. Appl. Phys. **86**, 6315 (1999).

[20] A. Giguere, M. Foldeaki, B. Ravi Gopal, R. Chahine, T. K. Bose, A. Frydman, and J. A. Barclay, Phys. Rev. Lett. **83**, 2262 (1999).

[21] M. Yue, J. Zhang, H. Zeng, H. Chen and X. B. Liu, J. Appl. Phys. **99**, 08Q104 (2006).

[22] L. Tocado, E. Palacios, and R. Burriel, J. Therm Anal. Calorim. **84**, 213 (2006).

[23] K. A. Gschneidner, Jr., V. K. Pecharsky, E. Brück, H. G. M. Duijn, and E. M. Levin, Phys. Rev. Lett. **85**, 4190 (2000).